Cement and Concrete Research 39 (2009) 981–988

Contents lists available at ScienceDirect

Cement and Concrete Research

journal homepage: http://ees.elsevier.com/CEMCON/default.asp

Re-examining the prospects of aluminous cements based on alkali-earth and rare-earth oxides[☆]

A.K. Chatterjee [*]

Conmat Technologies Pvt Ltd, Salt Lake, Kolkata, India

ARTICLE INFO

Article history:
Received 12 November 2008
Accepted 30 July 2009

Keywords:
BaO
Calcium aluminate cement
Refractory cement
Strontium compounds

ABSTRACT

In the family of aluminous cements the potential of strontium aluminate, the strontium–barium aluminate and the barium aluminate cements have been sporadically and incoherently studied over several decades in various parts of the world and more particularly in the East European countries without much wide-spread commercial success. Attempts had also been made to extend the exploratory studies to the (Ca, Sr, Ba)O–Al_2O_3–ZrO_2–HfO_2 system to synthesize super-refractory binders.

In fact, the above compositions, prima facie, seem to have the potential of arriving at cementitious formulations that, apart from being super-refractory, may as well be highly resistant to seawater, X-rays and gamma radiation. Looking at these potentials, quite a few experimental studies have been carried out under the guidance and supervision of the present author. The present paper is an endeavour to collate the data on some of these systems both from the published literature as well as from the author's findings. The prime motive has been to review and re-assess the prospects of manufacturing a range of new aluminous binders with superior properties.

1. Introduction

The discovery of calcium aluminates, the study of their crystal chemistry and phase equilibria, subsequently developing an alumina cements family and their ultimate field applications covered a span of one and a half centuries, although Bied received the French and the British patents for a method to produce a calcium alumina cement with bauxite and lime in a cupola furnace in 1908–1909, just about a century back.

Today there are three broad grades of calcium aluminate cements (CAC) of low, intermediate and high-purity, levels that include a wide range of compositions. They are manufactured in many countries and used for both refractory and non-refractory purposes.

Despite the long history and fairly extensive use of calcium aluminate cements, they display certain critical shortcomings in their hydration characteristics and application properties, some of which are illustrated below:

(i) Calcium aluminate (CA), which is the predominant phase in all CAC^s, melts incongruently at 1600 °C. Other aluminates with higher melting temperatures are essentially non-hydraulic. Castables made with CAC is mostly limited to uses up to 1600 °C or so.

(ii) Ambient temperatures can have a major effect on the behaviour of the binder, both during mixing and subsequent property development.

(iii) The hydration products generally show temperature and time-dependent conversion from CAH_{10}[1] to $C_2AH_8^1$ to $C_3AH_6^1$, resulting in volume change and strength retrogression.

Use of CAC in basic refractories is rather limited as it leads to the formation of low-melting compounds like monticellite. In certain non-refractory applications the CAC^s show comparatively poorer resistance to aggressive environments as well as to x-rays and gamma radiation. Considering the above shortcomings, studies had commenced almost six decades back if the alkali-earth oxides like SrO and BaO could replace lime in the synthesis of aluminates [1,2]. Later attempts were also made to expand the system of CaO–SrO–BaO–Al_2O_3 to include rare-earth oxides like ZrO_2+HfO_2 [3]. From the eighties the author was involved in a series of pilot-scale development of the new family of aluminous cements [4]. The present paper is an attempt to collate the available published and experimental data with a view to triggering re-exploration of the prospects of the new range of aluminous binders.

2. The binary systems

2.1. Strontia–alumina phase equilibria

The phase diagram of the strontia–alumina binary system was constructed as far back as 1959 (Fig. 1) [5]. Five binary aluminate

---

[☆] Presented at Calcium Aluminate Cements 2008: The Centenary Conference.

[*] Fax: +91 33 2334 7330.
E-mail address: anjan.k.chatterjee@gmail.com.

[1] C = CaO, A = Al_2O_3, H = H_2O.

0008-8846/$ – see front matter © 2009 Elsevier Ltd. All rights reserved.
doi:10.1016/j.cemconres.2009.07.027

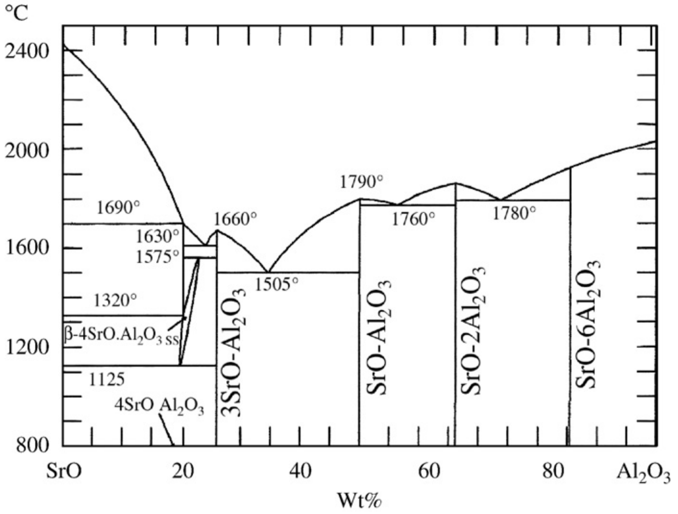

Fig. 1. The SrO–Al$_2$O$_3$ System (5).

phases were deciphered then: Sr$_4$A[2], Sr$_3$A[2], SrA[2],SrA$_2$[2] and SrA$_6$[2]. Compound Sr$_4$A showed two modifications: a high-temperature form (α-phase) stable in the range 1320 °C to 1690 °C and a low-temperature for (β-phase) stable from 1125 °C to 1320 °C. The low-temperature phase formed solid solution with alumina or Sr$_3$A.

Another compound Sr$_5$A was later reported [6]. It was obtained by sintering a stoichiometric mix of SrCO$_3$ and Al$_2$O$_3$ · H$_2$O at 1300 °C and at the same time the author failed to obtain SrA$_2$ even after repeated sintering of the mixes that yielded SrA + SrA$_6$ instead.

Later an attempt was made to re-ascertain the fusibility data of the system [7] (Fig. 2). Although the binary compounds were detected and their equilibria were more or less the same as in Fig. 1, the measured melting temperatures were significantly higher.

On the whole, it is interesting to observe that there are both similarities and differences between the strontia–alumina and lime–alumina systems, as briefly mentioned below:

(a) There are no compounds like Sr$_5$A and Sr$_4$A in the lime–alumina system.
(b) There is no analog of C$_{12}$A$_7$ in the strontia–alumina system.
(c) The similarities exist to some extent between Sr$_3$A and C$_3$A, SrA and CA, SrA$_2$ and CA$_2$ as well as between SrA$_6$ and CA$_6$, although the melting behaviour and temperature significantly differ.

2.1.1. Baryta–alumina phase equilibria

The phase diagram of the baryta–alumina system was reported first in 1952[8] and later in 1960[9] (Fig. 3). The main difference between these two diagrams lies in the melting point of B$_3$A[3] and the temperature of its two eutectics.

The presence of three binary compounds, viz., B$_3$A, BA and BA$_6$ was unequivocally established in both the studies. Attempts to synthesize other aluminate phases in this system did not meet with success [10].

The baryta–alumina system, therefore, shows distinct differences with the lime–alumina system in having three highly stable congruently melting binary aluminates that form rather flat binary eutectics with the adjacent compound, giving rise to stability of the phases at high temperatures.

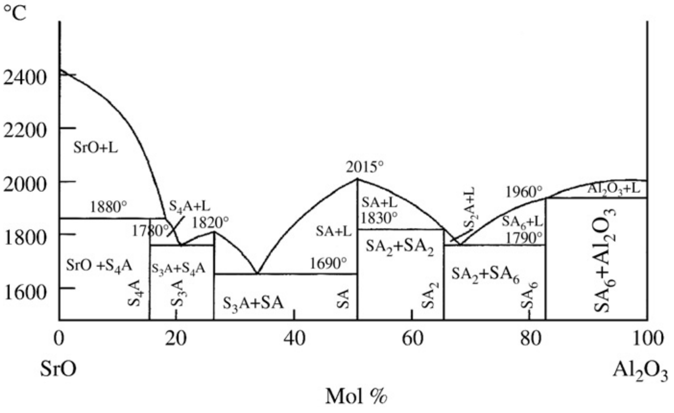

Fig. 2. The SrO–Al$_2$O$_3$ System (7).

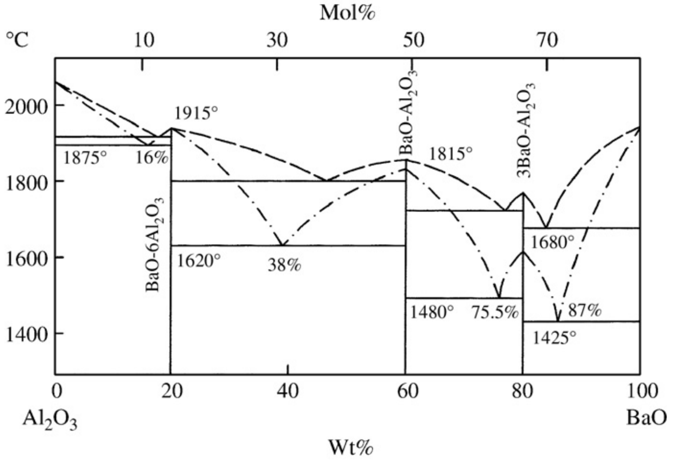

Fig. 3. The BaO–Al$_2$O$_3$ System (8,9).

3. Comparison of the monoaluminate phases

All the three alkali-earth monoaluminates, viz., CA, SrA and BA, being the primary cement-forming phases, deserve a careful

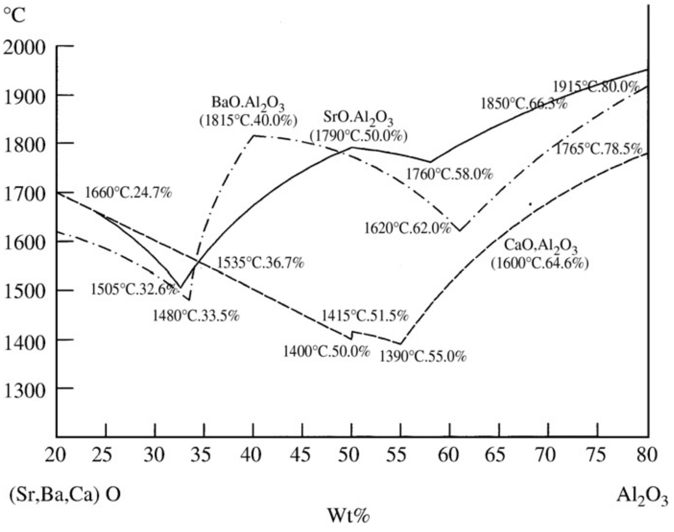

Fig. 4. Comparison of the liquidus curves around the monoaluminate phases (5,8,12).

---

[2] Sr = SrO, A = Al$_2$O$_3$.

[3] B = BaO, A = Al$_2$O$_3$.

Table 1
Comparison of the important parameters of the three aluminates.

Aluminates	Oxide components %		mol% wt	Density g/cm^3	Melting behaviour and temperature °C	Crystal system
	Alkali-earth oxide	Al_2O_3				
CA	35.4	64.6	157.96	2.96	Incongruent at 1600	Monoclinic
SrA	50.4	49.6	205.58	3.82	Congruent at 1790/2015[a]	Pseudo-hexagonal
BA	59.6	40.4	252.30	3.99	Congruent at 1815/1830[b]	Cubic

[a] Refs.: [5] and [7].
[b] Refs.: [8] and [9].

comparison. The melting temperatures of the phases, their stability at the melting stage and the liquidus patterns are compared in Fig. 4. It is obvious that the high-temperature stability of the phases is as follows:

BA > Sr A > CA

Further, the traces of the liquidus curves around SrA and BA are much flatter than the liquidus around the CA phase. Thus the compositional deviations in the cement from the CA line are more precarious for the CA cements than the compositional shifts in BA and SrA cements.

Some of the important parameters of these three aluminates are compared in Table 1.

4. The ternary systems

4.1. Lime–strontia–alumina phase relations

The studies on this ternary system have been reported in [11,12] and only the phase diagram from [12] is presented in Fig. 5. Prior to establishing the phase diagram, the subsolidus phase relations were determined at 1350°–1400 °C.

Complete solid solution was observed in all the sections CaO–SrO, C_3A–Sr_3A, CA–SrA, CA_2–SrA_2 and CA_6–SrA_6. Besides, a very small field of a ternary solid solution based on Sr_4A was detected.

The phase diagram of the ternary system as presented in Fig. 5 displays four ternary eutectics, viz., Q (1350 °C), N (1550 °C), O (1600 °C) and P (1620 °C), which lie virtually outside the stability field of (SrO, CaO) · Al_2O_3 solid solution phase. This implies that this solid solution phase has a wide field of high-temperature stability.

4.2. Lime–baryta–alumina phase relations

The subsolidus phase relations of this system at 1250 °C has been reported in [13], while the relations at 1400 °C have been published in [14] and reproduced in Fig. 6. As evident from the figure, there is a ternary compound C_2BA_4 in this system which is reportedly stable up to 1450 °C. At 1450 °C there is solid solubility of BA with CA up to only 7–8 mol%. Thus, in the lime-bearing ternary system, the stability field of BA is rather limited.

Thus, if one were to compare the effect of lime on BaO–Al_2O_3 and SrO–Al_2O_3 systems, it is evident that the effect is more pronounced in the CaO–BaO–Al_2O_3 system in bringing down the high-temperature stability of BA than on the SrA in the CaO–SrO–Al_2O_3 system.

5. Manufacturing issues for the new aluminate cements

For the high-purity aluminous cements the primary source of alumina is the calcined alumina from the Bayer's process. This obviously is the common raw material in the entire family of aluminous cements. While for CAC the source of lime is the high-purity limestone, for the

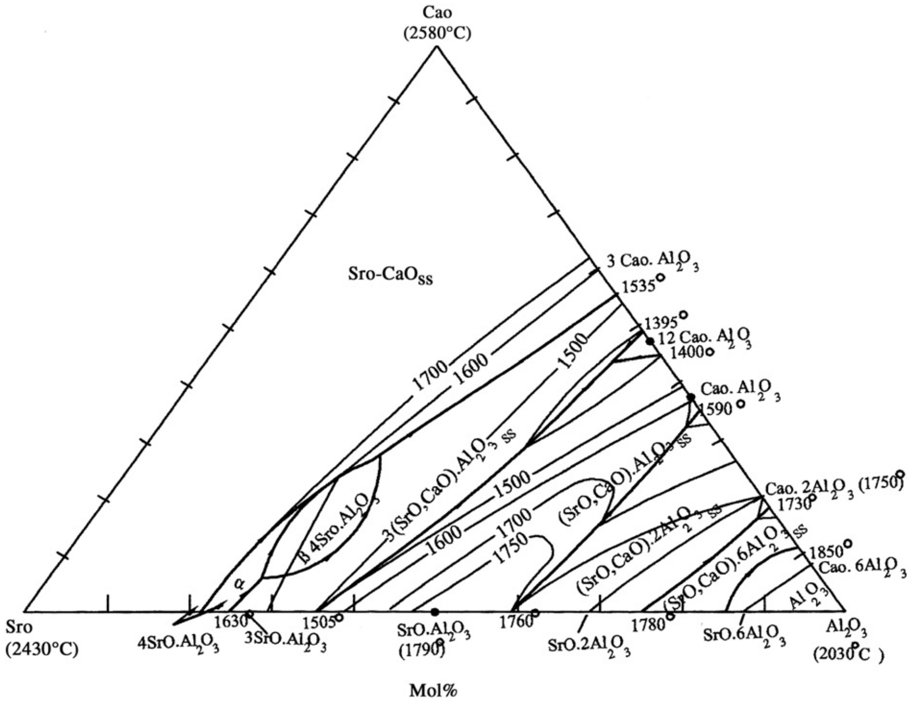

Fig. 5. The CaO–SrO–Al_2O_3 System (12).

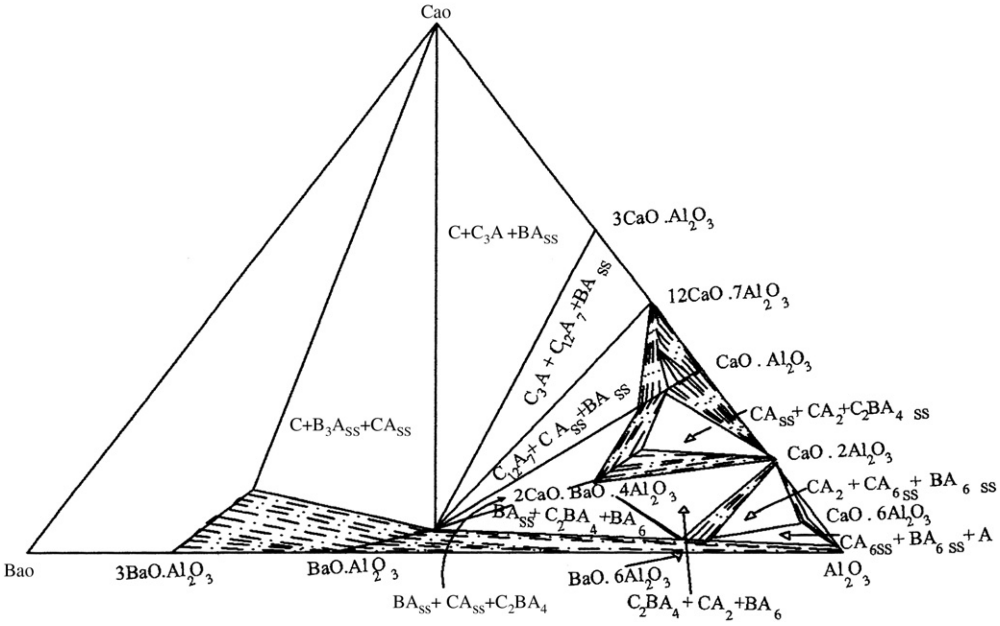

Fig. 6. The subsolidus phase relations in the system CaO–BaO–Al_2O_3 (13).

SrAC[4] and BAC[5] the raw materials are strontianite ($SrCO_3$) or celestite ($SrSO_4$) and witherite ($BaCO_3$) and barite ($BaSO_4$) respectively. The salient comparative characteristics of these natural mineral resources are summarized in Table 2.

It is perhaps relevant to note that the natural carbonate phases of strontium and barium are infrequent in occurrence and appear as minor sources of the alkali-earth oxides, while the corresponding sulphate forms occur more extensively and are used for extraction of relevant chemicals for industrial applications. However, our experience shows that in producing the aluminate cements, although the sulphate minerals are usable, they often required the use of reducing agents. In this context the carbonate forms of mineral are more amenable to easy decomposition. However, the presence of contaminants may call for the use of synthetically processed carbonates. In the pilot-scale studies reported in this paper the synthetic carbonates have been used as the raw materials (Table 3).

5.1. Pilot production process

For both BAC and SrAC the process adopted was based on cogrinding of the raw materials in required stoichiometric proportions in a ball will to a fineness of 5% residue on 212 µm. The ground raw mix was nodulised with water to about 15 mm size and the dried nodules were fed into a pilot rotary kiln. The sintering temperature was maintained at about 1620 °C and 1640 °C for the SrAC and BAC respectively. The clinker was air quenched and ground to 300 ± 10 m^2/kg and 280 ± 10 m^2/kg for SrAC and BAC respectively.

The cement compositions are given in Table 4. Both the cements showed the formation of predominantly monophasic aluminate phases.

6. Comparison of hydration mechanisms

It is well known that the hydration process of all the aluminate cements commences on initial contact of the binder with water. In the case of CAC, the primary reactions form crystalline calcium aluminate hydrates and a hydrated alumina present as either a crystal or a gel. The formation of the calcium aluminate hydrates, however, depends on the temperature at which the reaction occurs as summarized in Table 5.

It should be noted that even when substantial amounts of the hexagonal hydrates are formed initially, they may gradually dissolve and recrystallize as C_3AH_6 and AH_3, which are the thermodynamically stable forms. This conversion phenomenon occurs at all temperatures but is very sluggish at temperatures below 20 °C. At higher temperatures the rate increases and above 50 °C a paste becomes converted after one day. There is no doubt that conversion is a very important factor to be considered in all applications of CAC^s, and more particularly at ambient conditions.

Like CAC, the SrAC also displays hydraulic behaviour in contact with water and gets converted into distrontium aluminate hydrate (Sr_2AHn) and AH_3. No time- or temperature-dependent conversion phenomenon was detected in the preliminary hydration studies. However, more detailed investigations need to be undertaken to unravel the hydration behaviour of SrAC and more particularly, when the aluminate phase is made up of the (SrO, CaO) · Al_2O_3 solid solution series. The measurement of heat of hydration of this phase is yet to be carried out.

The BAC, however, is confirmed to be non-hydraulic to some extent, as in our studies one could ascertain its solubility in water by observing the expansion of standard cubes at the time of curing under the laboratory conditions of 18 °C and 90% Rh. With change in the curing procedure from the humidity chamber to airtight polythene bags, the testing difficulties due to water solubility were avoided. The hydration of BAC also displayed high heat of hydration (220 cal/g) after 24 h as well as flash setting.

The initiation of the hydration reactions occurs with leaching of Ba^{2+} ions and formation of hydroxides following the reaction:

$$\mathrm{BA} + 2\mathrm{H_2O} \rightarrow \mathrm{Ba}^{2+} + 2\mathrm{AlO}^{2-} + \mathrm{H_3O}^{+} + \mathrm{OH}^{-}$$

Under isolated curing with low w/b ratio the following reactions were noticed:

$$\mathrm{BA} + 6\mathrm{H} \rightarrow \mathrm{BAH_6}$$

$$2\mathrm{BAH_6} \rightarrow \mathrm{B_2AH_9} + 2\mathrm{AH_3}$$

$$\mathrm{B_2AH_9} + \mathrm{BA} \rightarrow \mathrm{B_3AH_6} + 2\mathrm{AH_3}$$

---

[4] Strontium aluminate cement.

[5] Barium aluminate cement.

Table 2
Comparative characteristics of the natural mineral resources used for SrAC and BAC production.

Characteristics	SrAC raw materials		BAC raw materials	
	Strontianite	Celestite	Witherite	Barite
Composition	$SrCO_3$ (SrO 70.1%)	Sr SO_4 (SrO 56.4%)	$BaCO_3$ (BaO 77.7%)	$BaSO_4$ (BaO 65.7%)
Crystal system	Orthorhombic	Orthorhombic	Orthorhombic	Orthorhombic
Hardness, H	3.5–4.0	3.0–3.5	3.0–3.75	2.5–3.5
Specific gravity, G	3.68–3.71	3.95–3.97	4.27–4.35	4.30–4.60
Contaminants	CaO	CaO, BaO	CaO, MgO	CaO
Mode of Occurrence	Veins in limestones, marls and also with eruptive rocks	Associated with limestone or sandstone; occurs also in beds of gypsum and rock salt	Veins associated with galena	Occurs with limestone or sandstone

On the whole, the hydration mechanism of BAC is quite complex and is yet to be fully deciphered. In the meantime for all practical purposes the following measures have evolved to overcome and contain the hydration-related problems:

- Optimizing the specific surface area
- Low w/b ratio
- Higher curing temperature
- Insulating from the atmosphere to the extent practicable
- Use of retarders like aluminium sulphate, alkali borate, zinc fluorosilicate, etc.

7. Combination of alkali-earth and rare-earth oxide systems

There has been a concept that suitable combinations of alkali-earth aluminates and rare-earth phases like zirconates and hafnates are likely to yield super-refractory compositions. Certain experimental validation of this concept has been reported in [4].

Before we come to these multicomponent systems, it may be worthwhile to recall that all the alkali-earth oxides react with ZrO_2 to form corresponding zirconates. The phase equilibria of $CaO–ZrO_2$ system is complicated at the zirconia end of the system due to the solubility of CaO in ZrO_2 at different temperature ranges, stabilizing different crystallographic systems. However the existence of $CaZrO_3$ was confirmed in 1929 [15] and reconfirmed later [16,17]. The compound was reported to be congruently melting at 2350 °C with density of 4.66 g/cm^3. There are differences of views regarding the crystal symmetry of the compound as to whether it belongs to the monoclinic or rhombohedral system.

Similarly in the $SrO–ZrO_2$ system the existence of $SrZrO_3$ was confirmed and reconfirmed by many researchers [18–20]. There are however, differences in the measurement of its melting point varying form 1650 °C to 2800 °C, although its congruently melting character and rhombohedral crystal symmetry are generally agreed upon. There are also differences of views regarding the stability and precise compositions of other binary compounds in the systems such as Sr_2ZrO_4, $Sr_5Zr_3O_{11}$ and $Sr_3Zr_3O_7$.

Table 3
Composition of the raw materials used in the pilot production.

Constituents	Calcined alumina	Processed strontium carbonate	Processed barium carbonate
LOI	0.80	28.8	21.40
SiO_2	0.04	0.60	0.50
Al_2O_3	98.80	–	–
Fe_2O_3	0.04	0.15	0.10
CaO	–	1.20	0.54
MgO	–	0.12	0.15
SrO	–	68.12	–
BaO	–	0.60	76.30
Na_2O	0.40	0.55	0.62
K_2O	<0.01	<0.01	<0.01

Table 4
Illustrative compositions of the aluminate cements produced.

Composition wt.%	SrAC	BAC
LOI	0.2	0.2
SiO_2	<1.0	0.4–1.0
Al_2O_3	46.0–48.0	38.5–39.5
Fe_2O_3	<0.4	0.1–04
CaO	<2.0	<2.0
SrO	52.0–54.0	–
BaO	<2.0	56.3–58.2
MgO	<0.2	<0.2
Na_2O	<0.5	<0.5
K_2O	<0.01	<0.01

Further, the $BaO–ZrO_2$ system is also known to have the existence of the binary compound $BaZrO_3$ [21] with congruent melting point of 2480 °C and density of 6.33 g/cm^3 [22]. Another hydraulically reactive phase Ba_2ZrO_4 has also been reported in this system [23].

Based on the above binary systems and the aluminous systems described earlier, one may examine the quaternary systems involving alkali-earth and rare-earth oxides. In the quaternary system $CaO–SrO–Al_2O_3–ZrO_2$ a large number of compatibility triangles can be delineated in the subsolidus state (Fig. 7). From the fusibility curves in the region $CaO \cdot Al_2O_3–CaO \cdot ZrO_2–SrO{\cdot}ZrO_2–SrO{\cdot}Al_2O_3$ (Fig. 8) it appears that a large number of super-refractory compositions can be derived from the field.

On the other hand, one may observe a limited number of compatibility triangles in the system $(SrBa)O–Al_2O_3–HfO_2–ZrO_2$ (Fig. 9). In this complex system the ternary field $BaO–ZrO_2–Al_2O_3$ deserves special attention from the fusibility isolines (Fig. 10). The compositions in the field $BaAl_2O_4–BaZrO_3–ZrO_2$ display very high fusibility characteristics.

In sintering studies with raw materials like barium carbonate, alumina and zirconia (associated with hafnium oxide) one could observe reactions in the temperature range of 900 °C to 1600 °C, which yielded barium aluminate and barium zirconate (hafnate). In this system the formation of $BaZrO_3$ was 1.5 times faster than that of $BaAl_2O_4$.

A similar study with strontium and/or calcium carbonate along with alumina and zirconia displayed an identical trend, although the rate of formation of the aluminate phase was 1.5 times faster than that of the zirconate phase.

In a large number of compositions containing aluminate and zirconate/hafnate, the hydraulic binding properties were observed. The hydration mechanisms tentatively followed the patterns of $SrAl_2O_4$ and $BaAl_2O_4$ described earlier. The alkali-earth aluminate hydrates tend to form a contact zone around the zirconates or hafnates, resulting in strong microzones. The simultaneous formation and availability of aluminous hydroxy gel in the matrix help in the growth and consolidation of the microstructure.

Table 5
Hydrated phases in CAC.

Reaction temperature °C	Phases formed	Water required for complete hydration
<24	CAH_{10} (metastable hexagonal prisms) + AHx (gel)	58%
>24 <35	C_2AH_8 (metastable hexagonal plates) + AHx + AH_3	32%
>35	C_3AH_6 (stable cubic trapezohedrals) + AH_3	23%

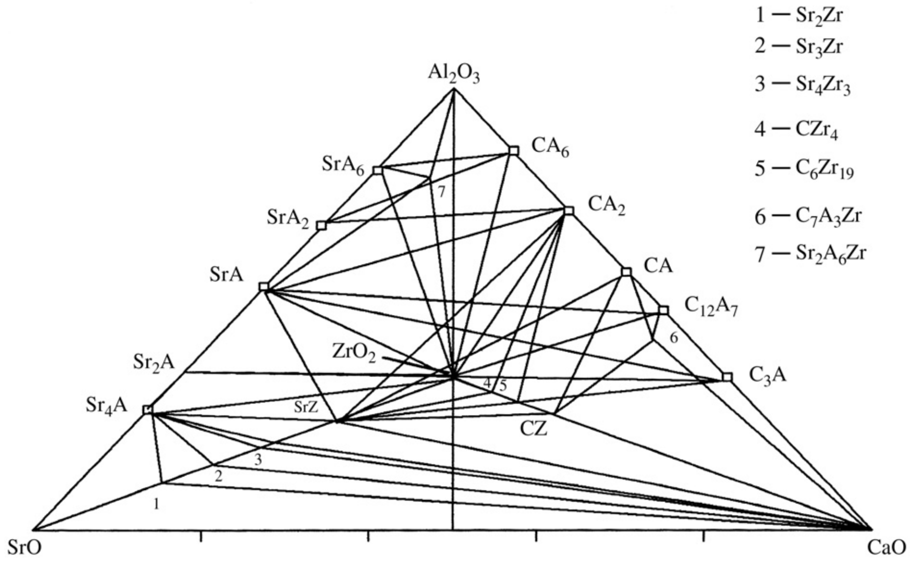

Fig. 7. The compatibility triangles in the system CaO–SrO–Al_2O_3–ZrO_2.

8. Exploring the low-temperature synthesis process for $BaAl_2O_4$

One of the major concerns in producing the alkali-earth aluminates is the requirement of very high sintering temperature. In order to overcome this problem a technology of low-temperature oxidation of Ba–Al powder mixtures was tried [24]. Mechanically alloyed Ba–Al precursor bars were exposed to pure flowing oxygen at 300 °C for 12 h, 550 °C for 24 h and then at 640 °C for 12 h. Appreciable formation of $BaAl_2O_4$ was detected after the heat-treatment at 550 °C along with a small amount of Al_4Ba, which on further oxidation at 640 °C, yielded further amount of the barium aluminate phase. Although this technology is at a preliminary stage of development, it may provide some clues for low-temperature synthesis of the refractory aluminate phases.

9. Application potential of the new aluminate cements

The application potential of the new aluminous cements was in the past examined from the three perspectives: refractory uses, seawater resistance and protection against X-rays and gamma radiations (1). On similar lines certain batches of pilot-produced cements were evaluated.

So far as the refractory applications are concerned, the properties of basic castables with chrome–magnesium co-clinker grains have been compared in Table 6, which clearly demonstrates the superiority of the Ba and Sr aluminate cements as compared to the calcium aluminate one.

It is evident from the table that one may certainly expect better performance of the $SrAl_2O_4$ and $BaAl_2O_4$ cements particularly as a binder in basic castables. The remarkable improvements in the hot modulus of rupture are particularly noteworthy.

The refractory performance of the aluminate–zirconate/hafnate composite cements appears to be even superior as illustrated in Table 7.

There are strong indications that strengths in excess of even 100 N/mm^2 might be achievable in the systems involving combinations of aluminates and zirconates with added advantages of very low shrinkage and insignificant loss of strength at intermediate temperatures when water is lost from the hydrate phases.

For non-refractory applications the new family of aluminous cements holds the potential of being used for making concretes for seawater resistance as well as for protections against radiation of X-rays and γ-rays. The comparative sulphate resistance tests were carried out

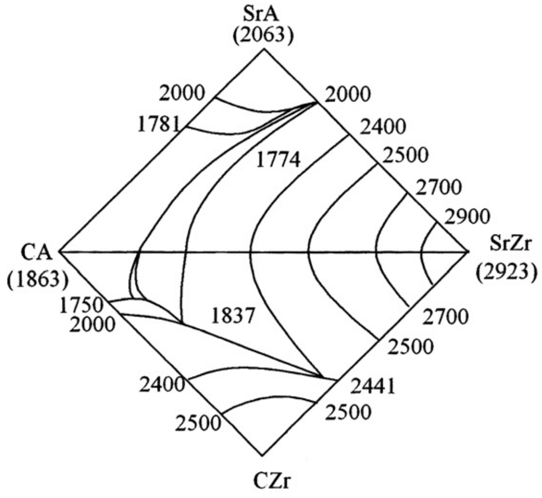

Fig. 8. Fusibility curves in the field CA–CZr–SrZr–SrA (°C).

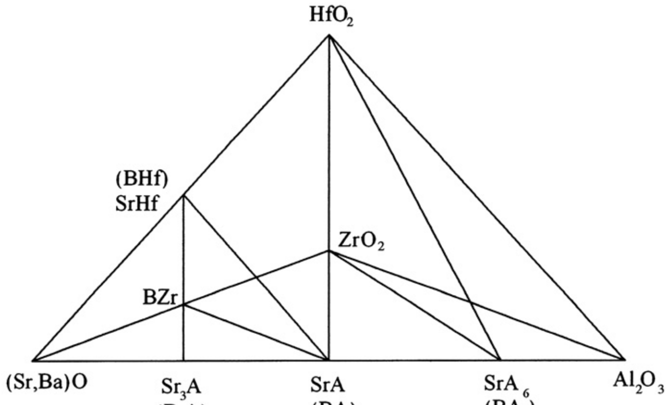

Fig. 9. The compatibility triangles in the system (Sr, Ba)O–Al_2O_3–HfO_2–ZrO_2.

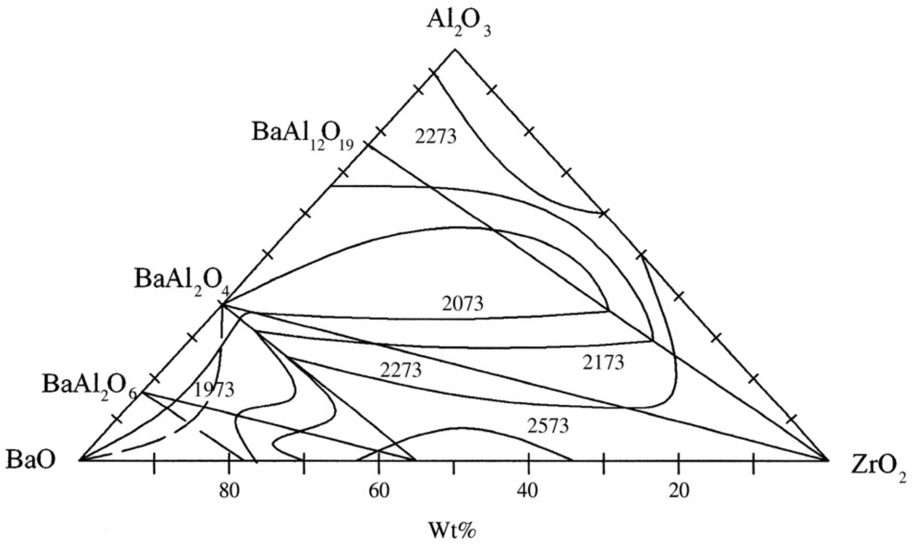

Fig 10. Fusibility curves in the field BaO–Al_20_3–ZrO_2 (°C).

for the aluminous cement mortars, which showed through expansion measurement and visual examination of prisms better resistance to sulphate attack as compared to calcium aluminate cements. In this context one may also note the long term trials carried out by Braniski in the Black Sea to establish the superiority of the strontium and barium aluminate cements with positive findings [1].

In a parallel study the same author had also established that the x-radiation protection capacity of barium aluminate concrete was almost at par with lead glass as borne by the following data [1].

Protective layer	Minimum thickness required in mm against the voltage of	
	60 kV	200 kV
Lead glass	8	34
BA–concrete	7	29

In the case of increasing intensities of X-radiation (say, up to 1000 kV) the barium aluminate concrete may turn out to be more cost-effective than lead glass.

The preliminary studies have also confirmed the earlier findings that the barium aluminate concrete has higher absorption coefficients for gamma radiation as well.

Table 6
Comparison of the properties of basic castables obtained with different aluminate cements under identical test conditions.

Properties	Cements		
	Calcium aluminate	Strontium aluminate	Barium aluminate
Bulk density, g/cm^3	2.63	2.72	2.78
CCS, N/mm^2 at			
110 °C	23	36	38
1100 °C	13	24	25
1550 °C	19	44	48
PLC% at 1550 °C	−0.75	−0.81	−0.81
Spalling resistance (850 °C to water)	8	14	14
HMOR, N/mm^2 at 1400 °C	1.6–1.8	4.2–4.9	4.6–4.8

10. Concluding remarks

It is not a new finding but it is a study of reconfirmation that a whole range of new aluminous cements based on strontium and barium oxides as well as from the combinations of aluminates and zirconates/hafnates can be formulated, synthesized and manufactured for more effective refractory and non-refractory applications than the widely used calcium aluminate cements.

Although the strontium aluminate cement is hydraulic in nature, it has not been studied to the same extent as the barium aluminate cement which is somewhat soluble in water and hence more difficult to handle. Notwithstanding the apparent shortcomings of the barium aluminate cement, it has been studied more extensively.

Since the strontium and barium aluminate cements have similar, though not identical, properties, more systematic and detailed comparative studies may unravel newer aluminous cements that would display higher refractory properties, higher resistance to thermal shocks, stronger resistance to environmental aggression, higher absorption of X-rays and γ-rays, etc.

There are further opportunities of expanding the horizon of alkali-earth aluminates by combining with rare-earth oxides to produce super-refractory materials.

Despite great prospects, there are issues of water solubility of barium, scarcity of raw materials, difficulties of synthesis, low working time for concrete, etc., which need to be resolved.

With more wide-scale concerted global research and development in foreseeable future one may see newer and more promising aluminous cements of great commercial value.

Table 7
Illustrative properties of alkali-earth/rare-earth oxide cements.

Properties	Binders			
	SrA–SrZ	SrA–SrHf	BA–BaZ	BA–BHf
Refractories, °C	2600	2670	2600	2400
CCS, N/mm^2	35	36	45	35
Compressive strength, N/mm^2 at				
1400 °C	40	40	49	40
1600 °C	50	52	52	42
Shrinkage % at 1800 °C	0.3	0.2	0.2	0.3

References

[1] A. Braniski, Barium and strontium cements, Zement-Kalk-Gips 5 (1957) 176–184.

[2] M. Drozdz, W. Wozek, Barium Aluminous Cement—Its Properties and Applications, Proc. Conference on Refractory Concretes, Karlovy Vary, Czech Republic, May 1974, pp. 1–17, (E 2512).

[3] Nicolaii Illyoukha and Valentina Timofeeva, Development of Hydraulic Zirconia Cements and Their Applications for Production of Refractories Items, Communication from the Academic Ceramic Centre, The Technical University, Kharkov, Ukraine, Personal Communication, 1998.

[4] D.G. Banawalikar, S. Narayanan, S.D. Majumdar, A.K. Chatterjee, New Generation Binders for Refractories, Proc. UNITECR III (1997) 1305–1314.

[5] M. Franco, System $SrO–Al_2O_3$, Chim. Ind. (Milan) 41 (1959) 114;
E.M. Levin, C.R. Robbins, H.F. McMurdie (Eds.), Phase Diagram for Ceramists, The AcerS, Ohio, USA, 1969, p. 118.

[6] P.S. Dear, Synthesis of strontium aluminates, Bull.-Va. Polytech. Inst. 50 (117) (1957);
N.A. Toropov, B.P. Barzakovskii, V.V. Lapin, N.N. Kurtseva (Eds.), Phase Diagrams of Silicate Systems, 1, Nauka Publishers, Leningrad, 1969, p. 221.

[7] M. Starszewski, Fusibility diagram of the system $SrO–Al_2O_3$, Zesz. Nauk. - Politech., Sl. 106 (1) (1964);
N.A. Toropov, B.P. Barzakovskii, V.V. Lapin, N.N. Kurtseva (Eds.), Phase Diagrams of Silicate Systems, 1, Nauka Publishers, Leningrad, 1969, p. 221.

[8] N.A. Toropov, F.Ya. Galakhov, Phase diagram of $BaO–Al_2O_3$ system, Dokl. Akad. Nauk SSSR 82 (1) (1952) 69;
N.A. Toropov, B.P. Barzakovskii, V.V. Lapin, N.N. Kurtseva (Eds.), Phase Diagrams of Silicate Systems, 1, Nauka Publishers, Leningrad, 1969, pp. 222–223.

[9] G. Purt, The $BaO–Al_2O_3$ system, Radex Rundsch. 4 (1960) 198;
N.A. Toropov, B.P. Barzakovskii, V.V. Lapin, N.N. Kurtseva (Eds.), Phase Diagrams of Silicate Systems, 1, Nauka Publishers, Leningrad, 1969, pp. 222–223.

[10] E. Calvert, H. Thibon, J. Dozoul, Synthesis of $2BaO–Al_2O_3$, Bull. Soc. Chim. Fr. 8 (1964) 1915.

[11] F. Massazza, M. Cannas, System $CaO–SrO–Al_2O_3$, subsolidus, Ann. Chim. (Rome) 49 (7–8) (1959) 1342–1350.

[12] F. Massazza, E. Sirchia, Phase equilibrium diagram of the system $CaO–SrO–Al_2O_3$ 49 (7–8) (1959) 1359–1369.

[13] C. Brisi, A. Appendino-Montorsi, Subsolidus phase equilibria in the system $CaO–BaO–Al_2O_3$ at 1250 °C, Ann. Chim. (Rome) 52 (9–10) (1962) 785–792.

[14] F. Massazza, Subsolidus phase equilibria in the system $CaO–BaO–Al_2O_3$ at 1400 °C, Ann. Chim. (Rome) 53 (7) (1963) 1002–1016.

[15] O. Ruff, F. Ebert, E. Stephan, Phase diagram of the system $CaO–ZrO_2$, Z. Anorg. Allg. Chem. 180 (3) (1929) 219.

[16] A. Dietzel, H. Tober, Phase relations in the system $CaO–ZrO_2$, Ber. Disch. Keram. Ges. 30 (3) (1953) 47.

[17] R. Roy, Partial phase diagram of the system $CaO–ZrO_2$, Bull. Soc. Chim. France 4 (1965) 1148.

[18] H. Wartenburg, W. Gurr, Studies in the system $SrO–ZrO_2$, Z. Anorg. Allg. Chem. 196 (4) (1931) 381.

[19] R.A. Tariopolskaya, N.V. Gulko, Tentative phase diagram of the system $SrO–ZrO_2$, Dokl. Acad. Nauk SSR 170 (5) (1966) 1140.

[20] A. Cocco, I. Chiacigh, Solid state reactions in the system $SrO–ZrO_2$, Ann. Chim. (Roma) 55 (12) (1965) 1341.

[21] E.K. Keler, N.A. Godina, Solid state reactions in the system $BaO–ZrO_2$, Ogneupory 18 (9) (1953) 416.

[22] E.K. Keler, A.K. Kuznetsov, Properties of barium zirconate, Zh. Prikland. Khimii 34 (10) (1961) 2146.

[23] Yu.M. Galkin, V.G. Chukhlantsev, Solid state reactions of BaO and ZrO_2, Izv. Acad. Nauk SSSR. Neorg. Mater. 1 (11) (1965) 1952.

[24] R. Citak, K.A. Rogers, K.H. Sandhage, Low-temperature synthesis of $BaAl_2O_4$/aluminum-bearing composites by the oxidation of solid metal-bearing precursors, J. Am. Ceram. Soc. 82 (1) (1999) 237–240.